2006

A generalized approach for the control of micro-electromechanical relays

Mohamed Abdelrahman Younis
Louisiana State University and Agricultural and Mechanical College, myouni1@lsu.edu

A GENERALIZED APPROACH FOR THE CONTROL OF MICRO-ELECTROMECHANICAL RELAYS

A Thesis

Submitted to the Graduate Faculty of the
Louisiana State University and
Agricultural and Mechanical College
in partial fulfillment of the
requirements for the degree of
Master of Science in Mechanical Engineering

in

The Department of Mechanical Engineering

by
Mohamed Younis
B.S., Mechanical Engineering, Louisiana State University, 2005
December, 2006

Acknowledgments

First of all, I thank God Almighty, the most gracious and the most merciful for everything I have been fortunate to have.

I am eternally indebted to my loving family in Egypt for their unending moral and financial support during the progress of my studies.

My sincere appreciation and thanks are given to my Major Professor, Dr. Marcio de Queiroz, for his patient academic guidance and constant input throughout the entire project and during successful compilation of this thesis. He has always held a generous open-door policy which I have exhausted. Dr. de Queiroz has been an excellent teacher and mentor during both my graduate as well as my undergraduate studies. I would also like to thank Dr. Yitshak Ram and Dr. Wanjun Wang for their willingness to serve as members on my examining committee. In addition, I would also like to extend my gratitude to my colleague Feng Gao for his kind assistance.

Finally, I would like to thank my friends for their continuous encouragement and support.

Table of Contents

List of Tables

List of Figures

Abstract

MEMS (Micro-Electromechanical Systems) is an area of research and applications that is becoming increasingly popular. It's mainly concerned with integrating micro-mechanical transducers with micro-electronic circuits on common substrates, traditionally silicon, through micro-fabrication. Instead of traditionally having the transducer and the communicating (or control) circuit as two separate entities, MEMS miniaturizes and combines them on a single chip, giving it several advantages, saving space, money, and increasing the sensitivity and accuracy of the integrated system.

A micro-electromechanical relay is a type of MEM devices that is becoming increasingly important in a wide range of industries such as the computer industry, the medical industry and the automotive industry, to name a few. However, micro-relays, both electrostatic and electromagnetic, share a common dynamic structure that causes an unfavorable phenomenon called *pull-in* in which the movable electrode comes crashing down to the fixed electrode once it reaches a certain gap spacing, possibly damaging the relay and creating undesirable output effects. To eliminate this phenomenon and have better control over the switching of the micro-relays, improving transient response and output error, a feedback control scheme is desired.

In this work, it is shown that voltage-controlled electromechanical micro-relays have a common dynamic structure allowing for the formulation of a generalized model. It is also shown that open-loop control of MEM relays naturally leads to pull-in during closing. An attempt has been made to control the relays eliminating this phenomenon and *tracking* a command signal that dictates the motion of the movable electrode over time with improved transient response. In doing so, two control schemes were adopted, a Lyapunov-based and a feedback linearization-based one.

Simulation results clearly show the superiority of the closed-loop control compared to the open-loop one. It's also shown that the Lyapunov-based controller was limited in the extent to which it

improved the transient response and that the feedback linearization-based controller performed much better. The latter eliminated pull-in and significantly lowered transient response and settling times, leading to very good tracking of the command signal.

Chapter 1: Introduction

Relays are used in a variety of industrial applications to open or close the connection in an electric circuit. Traditional mechanical relays, although large, slow, and noisy, are still widely used in various industrial control processes. Solid-state relays have much longer lifetimes, faster response, and smaller sizes than mechanical relays. However, solid-state relays generally have high on-resistance and low off-resistance, resulting in high-power consumption and poor electrical isolation, respectively. Design trade-offs for reducing their on-resistance tend to increase output capacitance, which introduces additional problems in applications involving the switching of high-frequency signals [20].

Micro-electromechanical systems (MEMS) technology has created opportunities for developing new types of signal and power relays [20]. Compared with solid-state relays, MEM relays have the same advantages as mechanical relays, namely, lower on-resistance, higher off-resistance, higher dielectric strength, lower power consumption, and lower cost. In addition, by using MEMS technology to miniaturize mechanical relays, the problems of size and switching time are treated. Finally, micro-relays can be integrated with other electronic components, as mentioned before.

MEM relays are split into two categories based on their method of actuation: electrostatic and electromagnetic [4,5,6,7,16,17,20]. Relays consist of two circuits, a control (or driving) circuit and an output (or driven) circuit. The basic composition and operation of mechanical relays will be discussed in more detail in Chapter 2. A picture of an actual electromagnetic micro-relay is shown here in Figure 1.1 [20].

The most common actuation method for micro-relays is electrostatic [20]. This is mostly due to difficulties in fabricating micro-size electromagnetic actuators. Another disadvantage is that electromagnetic actuation requires larger current, which leads to larger power consumption and larger

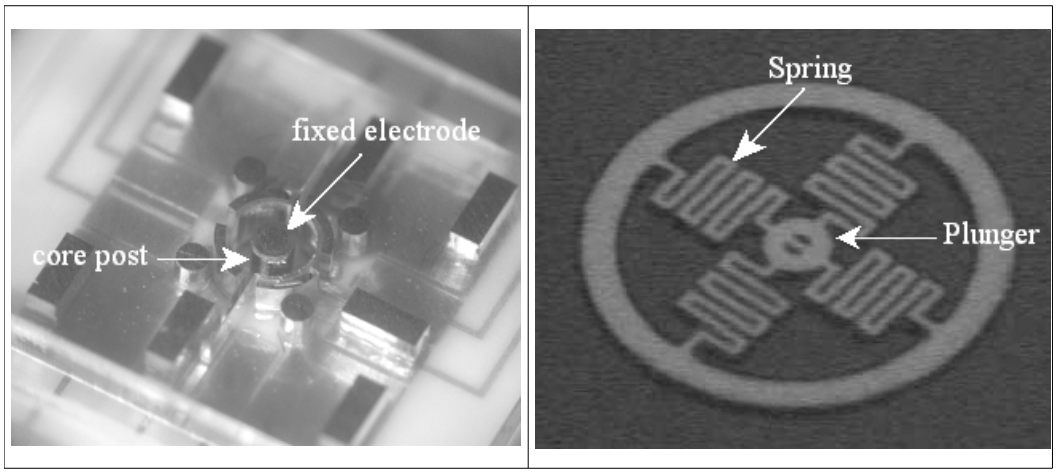

Figure 1.1. A picture of an electromagnetic micro-relay: bottom part (left) and top part (right) [picture used with permission of Dr. Wanjun Wang]

heat generation. Nevertheless, Busch-Vishniac examines both actuation methods in their ability to achieve micron and submicron precision in rapid motion, and concludes that there is a strong case to be made in favor of magnetically-driven micro-actuators [4]. For a more detailed literature review of the design and fabrication of electrostatic and electromagnetic micro-relays, the reader should consult the works of Jeong [7] and Williams [20], respectively.

Another split comes in the choice of the control-parameter of the relay. Electrostatic relays are usually voltage-controlled and their electromagnetic counterparts are usually current-controlled. Voltage-control has several advantages over current-control, namely, easier fabrication, faster operation, and reduced energy losses due to resistive heating [4]. This is partly responsible for electrostatic actuation being more dominant, and this is exactly why voltage-control was chosen for implementation in the control approach illustrated in this work.

Voltage-controlled MEM actuators exhibit an important nonlinear phenomenon called pull-in [10,12,15,18]. Mathematically, pull-in is associated with a saddle-node bifurcation [10]. Pull-in can be physically explained as follows. Suppose the voltage across the MEM actuator is incrementally increased from zero. At first, the electromechanical force will incrementally pull the movable electrode downward with increasing voltage. When the voltage reaches a critical value,

corresponding to an electrode displacement equal to 1/3 of the nominal (zero-voltage) gap, the movable electrode suddenly crashes into the bottom electrode. In MEM relays, this problem is especially detrimental since they are necessarily operated within the pull-in region of the gap when the relay closes. Obviously, repeated occurrence of pull-in will eventually damage the micro-relay.

To date, the application of control schemes to MEMS has lagged in development when compared to MEMS fabrication and structure design [19]. Few involve the control aspect in their research, and of those few, most MEM actuator control work has been devoted to the electrostatic case only. In [10,11,12], partial-state feedback control strategies were proposed using position and charge feedback and a velocity observer. Control schemes based on differential flatness, control Lyapunov functions, backstepping, and input-to-state stabilization were reported in [21,22]. PD-type controllers were developed in [1,2] to control a 1 D.O.F. magnetically-levitated micro-suspension system and an electrostatically-actuated MEM optical switch, respectively.

Chapter 2: Micro-Relay Modeling

The following sections describe how voltage-actuated electrostatic and electromagnetic micro-relays operate. In addition, a mathematical model of each case is formulated.

2.1: Electrostatic Micro-Relay

2.1.1: Operation

In this work, only *normally-open* relays are being considered, i.e., ones in which the output circuit is open when no voltage is applied, and vice versa. In electrostatic relays, both circuits share a pair of parallel plates which are normally separated by a gap. However, once a voltage is applied in the control circuit, an electric field is generated between the two plates due to the potential difference, creating an attractive electrostatic (or capacitive) force between the plates which pulls them together (Figure 2.1). Once that happens, the two electrodes of the output circuit also come together allowing for the flow of current and closing the circuit. Usually, there is an isolating layer integrated into the electrodes to prevent the two circuits from interfering with each other. This feature is omitted in Figures 2.1 and 2.3 for simplicity. Once the voltage source is disconnected, the parallel plates (or capacitor) begin to discharge until the electrostatic force drops below its opposing spring force and the relay opens once again disconnecting both circuits.

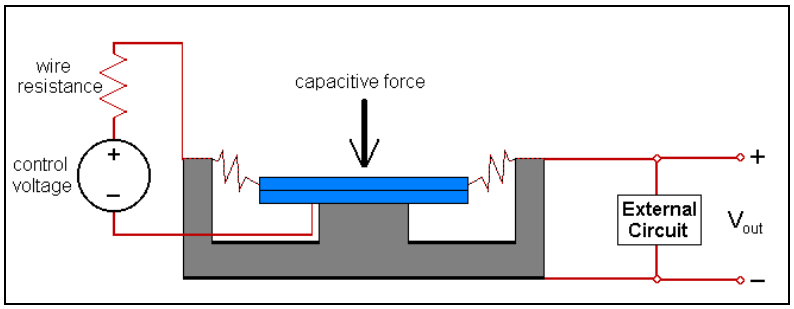

Figure 2.1. A diagram of an electrostatic micro-relay

2.1.2: Model

Figure 2.2 below is a diagram of a simple model of an electrostatic micro-relay and will be used to illustrate the forces acting on the plunger and define the parameters used in the mathematical formulation.

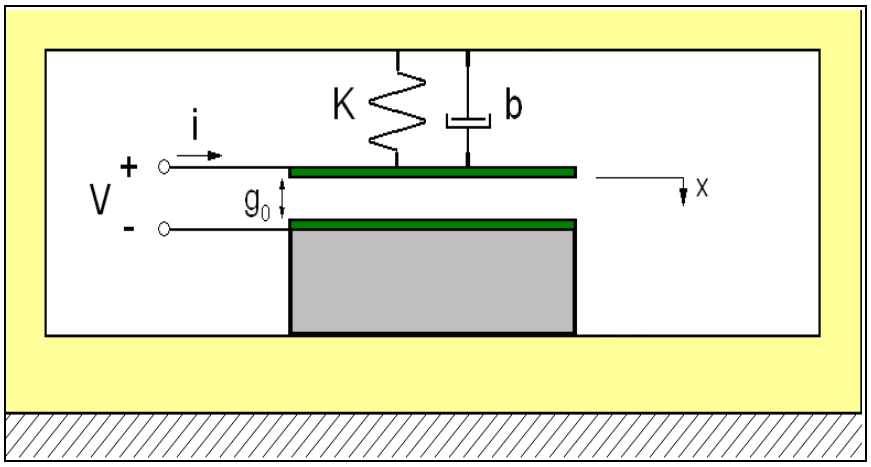

Figure 2.2. A simple electrostatic micro-relay model

As can be seen from Figure 2.2, the forces acting on the movable top plate, the *plunger*, are three, namely, the spring force, the damping force (resulting from the air damping effects), and the attractive electrostatic force. The latter is defined by Senturia in [18] as

$$F_{electrostatic} = \frac{q^2}{2\epsilon A} \tag{1}$$

where

q : the electrostatic charge built up in the capacitor
ϵ : the permittivity of free space
A : the cross-sectional area of the plunger

Summing the forces that act on the plunger such that acceleration is positive in the direction of increasing displacement, x, as shown in Figure 2.2 above, results in equation (2) for the mechanical subsystem.

$$m\ddot{x} + b\dot{x} + kx = \frac{q^2}{2\epsilon A} \tag{2}$$

where

m : the mass of the plunger
b : the damping coefficient
k : the spring stiffness

Observing Figure 2.2, one realizes that the total voltage drop through the electrical subsystem is compromised of one due to wire resistance and another due to the potential difference across the gap between the parallel plates. The latter is defined by Busch-Vishniac in [3] as

$$\Delta V_{capacitor} = \frac{g}{\epsilon A} q \tag{3}$$

where

g : the gap between the plates (g_0-x)
g_0 : the original gap (fully-open position)

Kirchoff's Voltage Law can now be used to obtain the following equation for the electrical subsystem:

$$V - iR - \frac{(g_0 - x)}{\epsilon A} q = 0 \tag{4}$$

where

V : the voltage supplied to the control circuit
i : the current induced in the control circuit

Equations (2) and (4) are combined to form the coupled system representation of the electrostatic micro-relay as shown in equations (5).

$$m\ddot{x} + b\dot{x} + kx = \frac{q^2}{2\epsilon A} \tag{5a}$$

$$R\dot{q} + \frac{(g_0 - x)}{\epsilon A} q = V \tag{5b}$$

2.2: Electromagnetic Micro-Relay

2.2.1: Operation

In electromagnetic relays, a control circuit that consists of electrical wire wound into a coil around a central post is used to generate a magnetic field by running a current through the wire. The resulting magnetic force then acts on the plunger situated above the post attracting it and closing the output circuit (Figure 2.3) in the same manner as previously described with regards to the electrostatic relay. Similarly, once the voltage source is disconnected, the magnetic flux begins to diminish until the spring force can overcome the electromagnetic force, opening the relay.

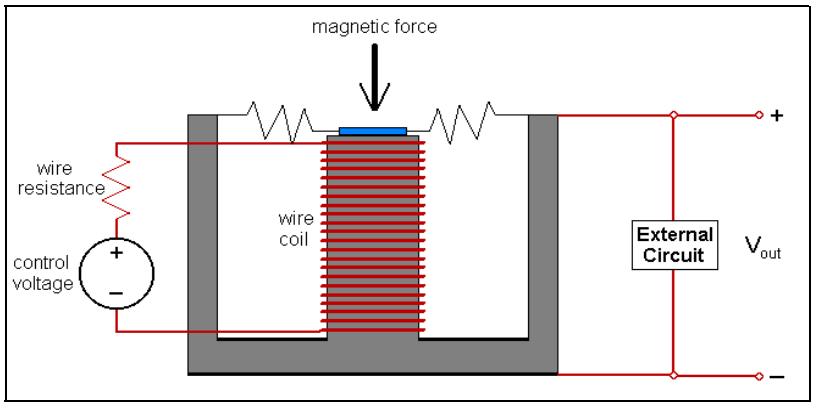

Figure 2.3. A diagram of an electromagnetic micro-relay

2.2.2: Model

Figure 2.4 is a diagram of a simple model of an electromagnetic micro-relay and will be used to illustrate the forces acting on the plunger and define the parameters used in the mathematical formulation. Note that the red shading and the multi-colored dashed outlines were done for analysis purposes only and are to be ignored for the purpose of this work.

It is apparent that a force summation will be similar to the electrostatic case described previously with the only exception being the presence of an electromagnetic force as opposed to an electrostatic one. The electromagnetic force is defined in [3] as shown in (6).

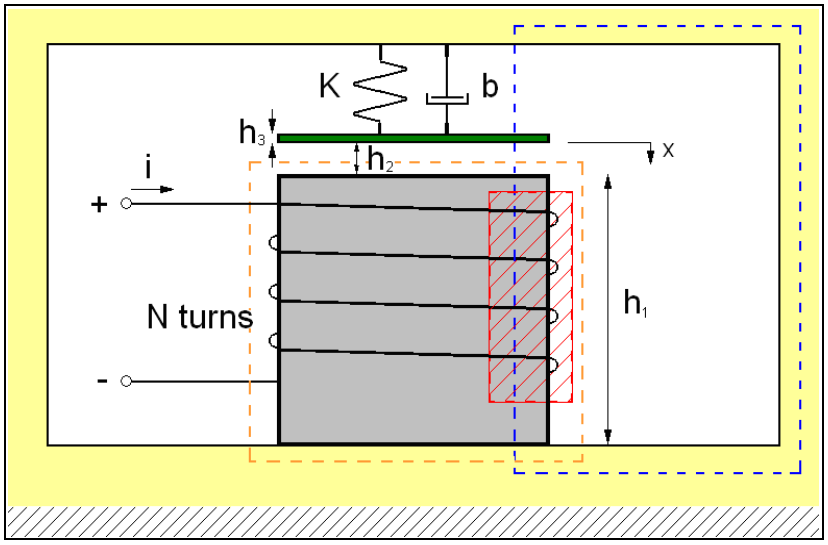

Figure 2.4. A simple electromagnetic micro-relay model

$$F_{electromagnetic} := \frac{1}{2\mu_0 A}\left(\frac{N i}{\Re(x)}\right)^2 \tag{6}$$

where

μ_0 : the permeability of free space

N : the number of coil turns around the central post

$\Re(x)$: the reluctance of the magnetic circuit

The reluctance of the magnetic circuit is defined in [20] as

$$\Re(x) = \frac{1}{A}\left[\frac{h_1}{\mu_1} + \frac{(g_0 - x)}{\mu_0} + \frac{h_3}{\mu_3}\right] \tag{7}$$

where

h_1 : the height of the core post

μ_1 : the permeability of the core post's material

h_3 : the thickness of the plunger

μ_3 : the permeability of the plunger's material

It was shown that the first and third terms in the reluctance expression shown in (7) are negligible, compared to the second term. This is due to the permeabilities of the mentioned terms being significantly larger than that of free space. Rewriting (7), after simplifying and dropping the subscripts, yields (8).

$$\Re(x)=\frac{(g_0-x)}{\mu A} \tag{8}$$

The electromagnetic force can now be rewritten in terms of the magnetic flux, ϕ , noting that

$$\phi=\frac{N i}{\Re(x)} \tag{9}$$

Substituting for ϕ from (9) into (6) results in the following expression for the electromagnetic force:

$$F_{electromagnetic}=\frac{\phi^2}{2\mu A} \tag{10}$$

Summing the forces that act on the plunger results in the following equation for the mechanical subsystem:

$$m\ddot{x}+b\dot{x}+kx=\frac{\phi^2}{2\mu A} \tag{11}$$

Now turning to the electrical subsystem and performing Kirchoff's Voltage Law should result in the dynamic equation, completing the model. The *terminal voltage* of the control circuit is needed, which is defined as the voltage drop through the coil due strictly to changes in the magnetic flux and not due to wire resistance. In [3], Busch-Vishniac defines this as (12).

$$\upsilon=\frac{d\lambda}{dt}=\frac{d(N\phi)}{dt}=N\dot{\phi} \tag{12}$$

where λ is the flux linkage of the circuit.

The voltage drop caused by the wire resistance can be rewritten, using Equation (9), as

$$\Delta V_{resistance}:=Ri=\frac{R\Re(x)}{N}\phi \tag{13}$$

Substituting for $\Re(x)$ from Equation (8), and applying Kirchoff's Voltage Law yields equation (14) for the electrical subsystem.

$$N\dot{\phi}+\frac{R(g_0-x)}{N\mu A}\phi=V \tag{14}$$

Equations (11) and (14) are combined to form the coupled system representation of the electromagnetic micro-relay as shown in equations (15).

$$m\ddot{x}+b\dot{x}+kx = \frac{\phi^2}{2\mu A} \tag{15a}$$

$$N\dot{\phi}+\frac{R(g_0-x)}{N\mu A}\phi = V \tag{15b}$$

2.3: Generalized Model

In an attempt to make a generalized model which would include both the electrostatic and the electromagnetic micro-relays, equations (5) and (15) have been manipulated enough to have the same basic structure. The new generalized model is now written as (16).

$$m\ddot{x}+b\dot{x}+kx = \alpha z^2 \tag{16a}$$

$$\beta\dot{z}+\gamma(g_0-x)z = u \tag{16b}$$

$$y = x \tag{16c}$$

where

$$z=\begin{Bmatrix} q \\ \phi \end{Bmatrix} \quad \beta=\begin{Bmatrix} R \\ N \end{Bmatrix} \quad \alpha=\begin{Bmatrix} 1/2\epsilon A \\ 1/2\mu A \end{Bmatrix} \quad \gamma=\begin{Bmatrix} 1/\epsilon A \\ R/(N\mu A) \end{Bmatrix} \tag{16d}$$

and the 1st and 2nd rows correspond to the electrostatic and electromagnetic cases respectively.

Note that (16) models the micro-relay dynamics only when there is no contact between the electrodes, i.e., $x\in(-\infty, g_0)$. When contact occurs, the kinetic energy of the movable electrode is assumed to become zero so that there is no bouncing of the movable electrode on the fixed electrode. For a dynamic model that includes contact bounce, the reader should consult [15].

Chapter 3: Open-Loop Operation

In this section, it is shown that open-loop operation of the micro-relays results in the unfavorable pull-in phenomenon and in very minimal control over the performance.

3.1: Pull-In Analysis

The following analysis is based on the one presented in [18] for an electrostatic micro-actuator. However, the analysis here is generalized to include both electrostatic and electromagnetic micro-relays.

From Equation (16), it is easily seen that the equilibrium conditions are given by $\dot{x}=0$, $\alpha z^2=kx$, and $h(x)z=u$, where $h(x)=\gamma(g_0-x)$. Ignoring the damping effects for the purpose of this analysis, the net force is defined as

$$F_{net}:=\alpha z^2-kx=\frac{\alpha u^2}{\gamma^2(g_0-x)^2}-kx \tag{17}$$

For the relay to be stable at a certain equilibrium, any slight perturbation in one direction or the other of that equilibrium position should not result in the system diverting further and further from equilibrium.

Naturally, F_{net} = 0 at the equilibrium point. Since the net force is defined in the direction of increasing electrode displacement, a positive net force will pull the movable electrode towards the fixed one. Therefore, a small change in the net force will affect stability in the manner illustrated in (18).

$$\begin{aligned} &\frac{\partial F_{net}}{\partial x}>0 && \rightarrow && \text{unstable equilibrium point} \\ &\frac{\partial F_{net}}{\partial x}<0 && \rightarrow && \text{asymptotically stable equilibrium point} \end{aligned} \tag{18}$$

It follows from (17) and (18) that the stability condition is given by:

$$u < \sqrt{\frac{\gamma^2 k (g_0 - x)^3}{2\alpha}} \tag{19}$$

Pull-in begins when the equilibrium point is at the stability threshold. Therefore, the following two conditions must be satisfied at pull-in:

$$F_{net} = 0 \quad \text{and} \quad u_{pi} = \sqrt{\frac{\gamma^2 k (g_0 - x_{pi})^3}{2\alpha}} \tag{20}$$

From (17) and (20), it is determined that pull-in occurs when

$$x_{pi} = \frac{g_0}{3} \quad \text{and} \quad u_{pi} = \sqrt{\frac{4\gamma^2 k\, g_0^{\,3}}{27\alpha}} \tag{21}$$

The above analysis has the following implication on the micro-relay operation when one attempts to close it by open-loop control. Suppose one incrementally increases the input voltage starting from zero, always allowing transients in the electrode position to die out [9]. When $u < u_{pi}$, the equilibrium position will increase from zero to $g_0/3$ while remaining asymptotically stable. When $u > u_{pi}$, the equilibrium position loses its stability and the movable electrode crashes into the bottom one. Thus, the set $\{x : g_0/3 < x \leq g_0\}$ is located in an unstable region of the open-loop system. Since during closing, the desired position of the micro-relay is inside this set ($x = g_0$), one cannot operate the micro-relay in an open-loop manner. This is demonstrated next through simulations of an electrostatic and an electromagnetic micro-relay.

3.2: Simulation Results

The parameters for the electrostatic micro-relay model used in all simulations, shown in Table 3.1, were taken from [14].

While performing the simulations, in order to account for the contact-bounce issue discussed earlier, the implementation strategy for the system dynamics presented in [18] is used. Using (16d)

Table 3.1. Electrostatic open-loop simulation parameters

m	=	1
k	=	1
b	=	0.2
g_0	=	1
A	=	100
ϵ	=	1
R	=	0.001

and (21), the pull-in voltage was found to be u_{pi} = 0.0544, 0.0003070 for the electrostatic and the electromagnetic cases, respectively.

Let y_d denote the desired position of the movable electrode. The goal is to operate the system according to the following function

$$y_d(t)=\left\{\begin{matrix} g_0 : 0\leqslant t<100 \\ 0 : 100\leqslant t<200 \end{matrix}\right\}, \quad y_d(t+200) = y_d(t) \tag{22}$$

which alternates the closing and opening of the micro-relay. A voltage that commands the micro-relay according to (22) is given by (23).

$$u(t)=\left\{\begin{matrix} 0.01\mathrm{t} : 0\leqslant t<50 \\ 1-0.01\mathrm{t} : 50\leqslant t<100 \\ 0 : 100\leqslant t<200 \end{matrix}\right\}, \quad u(t+200) = u(t) \tag{23}$$

The simulation results for the open-loop micro-relay are shown in Figure 3.1, where $g_{pi} = 2g_0/3$. Notice that when the voltage reaches the pull-in value, the movable electrode suddenly crashes into the fixed electrode. On the other hand, the movable electrode is not released until well after the voltage command is set to zero. This delay occurs because the charge in the capacitor builds up significantly during the pull-in, and then takes a while to discharge through the resistor (Figure 3.1) until the spring force overcomes the capacitive force. A similar simulation is performed for the electromagnetic case using the parameters in Table 3.2.

Table 3.2. Electromagnetic open-loop simulation parameters

m	=	1
k	=	1
b	=	0.2
g_0	=	1
A	=	100
ϵ	=	1
R	=	0.001
μ	=	$4\pi\times10^{-6}$
N	=	50

The resulting simulation gave similar results as shown in Figure 3.2. It is obvious from the figure that the coil takes even longer to discharge than the parallel plates in the electrostatic case. This is why the voltage command was modified from (23) to have a period of 300 rather than 200 seconds. This further emphasizes the need for a feedback controller for the operation of these micro-relays.

In light of the poor performance of the open-loop micro-relay, the goal in the next two chapters is to design a feedback control law, $u=u(x,\dot{x},z)$, such that the MEM relay can properly open and close with adequate control over the motion of the plunger and without damage to the device.

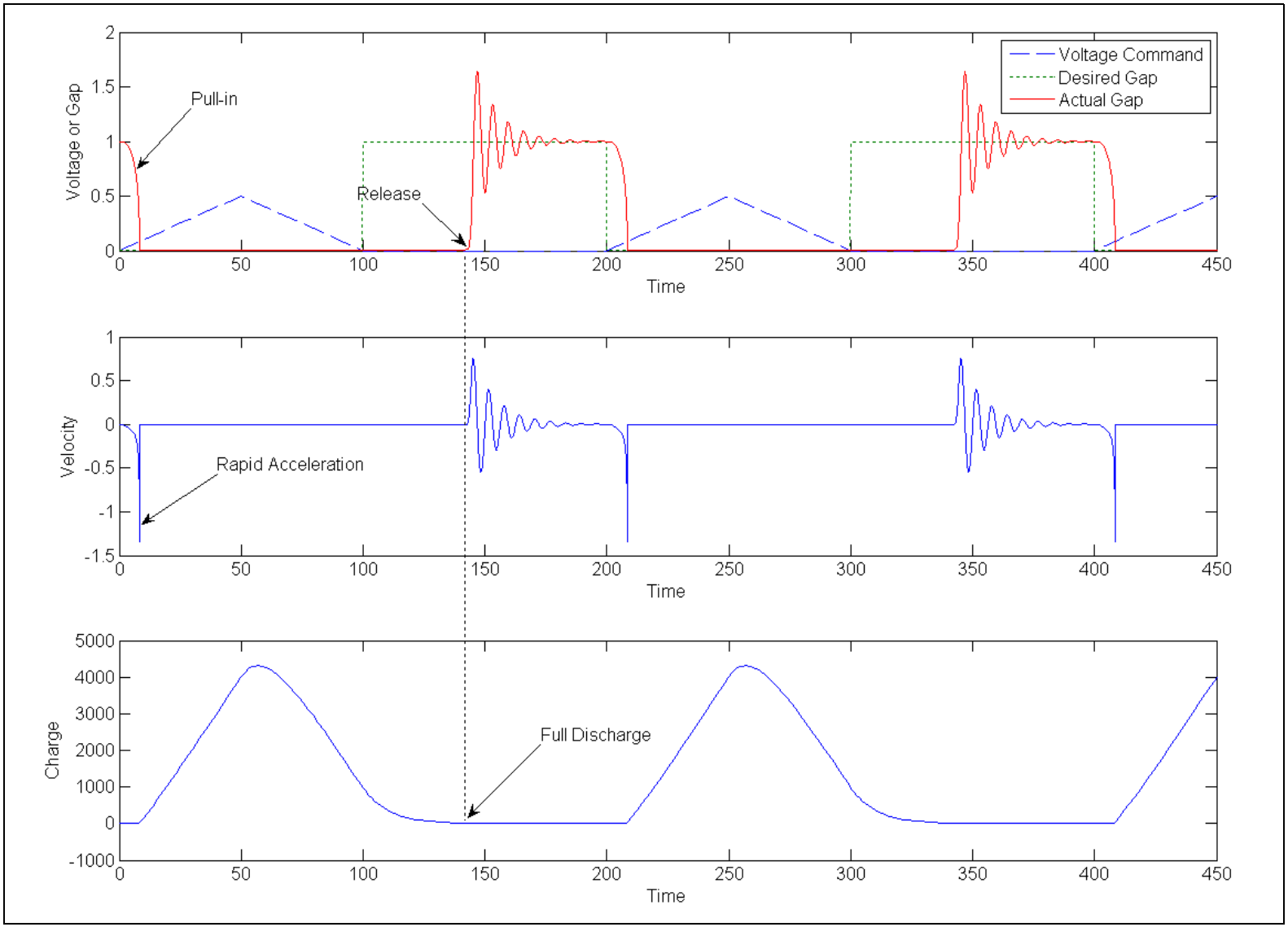

Figure 3.1. Electrostatic micro-relay open-loop operation

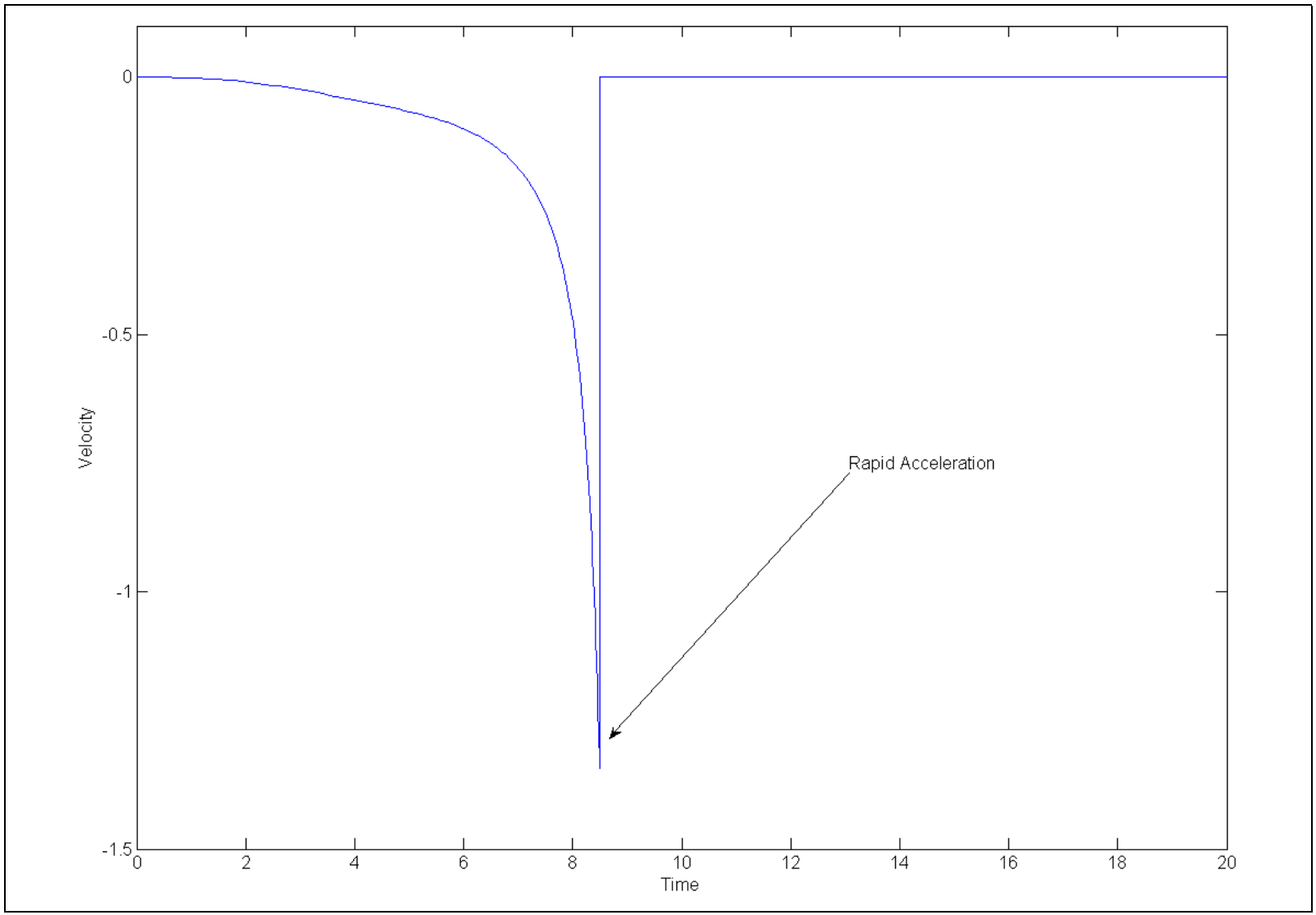

Figure 3.2. A close-up of the velocity of the plunger of the electrostatic micro-relay during open-loop operation. Pull-in is readily apparent.

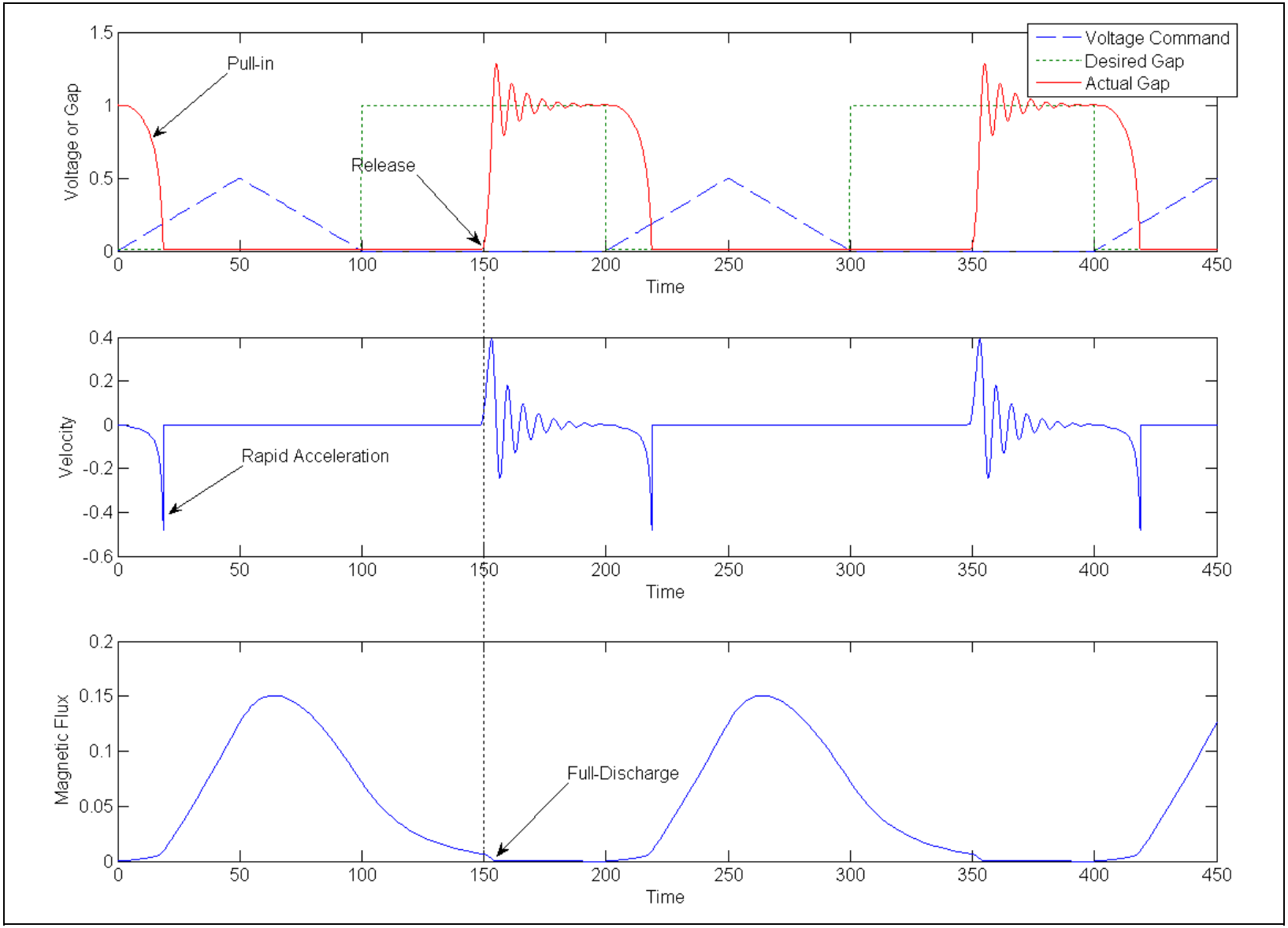

Figure 3.3. Electromagnetic micro-relay open-loop operation

Chapter 4: Lyapunov-Based Control

In this section, a feedback controller for the generalized MEM relay model (16) is constructed using a Lyapunov approach [8,9].

4.1: Control Synthesis

The control design will be done separately for the micro-relay closing and opening cycles.

4.1.1: Closing Cycle

In order to close the relay, the desired position is denoted by $y_d = g_0 > 0$ and the position error is represented by $e := y - y_d$. The objective is to ensure that $\lim_{t\to\infty} e(t)=0$. It follows that (16a) can be rewritten as

$$m\ddot{e}+b\dot{e}+ke+ky_d=\alpha z_d{}^2+\alpha(z+z_d)\eta \tag{24}$$

where z_d denotes a stabilizing function to be designed next and $\eta := (z - z_d)$. We set the stabilizing function to

$$z_d=\sqrt{\frac{1}{\alpha}\left(ky_d-c_1\tanh(e)-c_2\tanh(\dot{e})\right)} \tag{25}$$

where c_1 and c_2 are positive gains satisfying $c_1 + c_2 < ky_d$

Now, taking the derivative of η yields the equation shown in (26).

$$\beta\dot{\eta}=u-\gamma(g_0-x)z-\beta\dot{z_d} \tag{26}$$

where

$$\dot{z_d}=\frac{-1}{2\alpha z_d}\left[\frac{c_1}{\cosh^2(e)}\dot{e}+\frac{c_2}{m\cosh^2(\dot{e})}\ddot{e}\right] \tag{27}$$

The control input is then designed as

$$u=-c_3\eta+\gamma(g_0-x)z+\beta\dot{z_d}-\alpha(z+z_d)\dot{e} \tag{28}$$

where $c_3 > 0$.

Consider the positive-definite, radially-unbounded function shown in (29).

$$V = \frac{1}{2} m \dot{e}^2 + \frac{1}{2} k e^2 + c_1 \ln(\cosh(e)) + \frac{1}{2} \beta \eta^2 \tag{29}$$

The time derivative of (29) along (24) and (26) in closed loop with (25) and (28) yields the following negative semi-definite function:

$$\dot{V} = -b \dot{e}^2 - c_2 \dot{e} \tanh(\dot{e}) - c_3 \eta^2 \tag{30}$$

Given that $(e, \dot{e}, \eta) = 0$ is a unique equilibrium point of the closed-loop system, it follows from (29), (30), and LaSalle's theorem [8], that $(e, \dot{e}, \eta) = 0$ is asymptotically stable.

4.1.2: Opening Cycle

During the micro-relay opening, $y_d = 0$. It follows that (16a) and (16b) can be rewritten as (31) and (32) respectively.

$$m \ddot{e} + b \dot{e} + ke = \alpha z^2 \tag{31}$$

$$\beta \dot{z} = u - \gamma (g_0 - x) z \tag{32}$$

The control input is then designed as

$$u = -c_3 z + \gamma (g_0 - x) z - \alpha z \dot{e} \tag{33}$$

where $c_3 > 0$.

Taking the time derivative of the following positive-definite, radially-unbounded function in (34) along (31) and (32) in closed-loop with (33), yields the negative semi-definite function in (35).

$$V = \frac{1}{2} m \dot{e}^2 + \frac{1}{2} k e^2 + \frac{1}{2} \beta z^2 \tag{34}$$

$$\dot{V} = -b \dot{e}^2 - c_3 z^2 \tag{35}$$

Again, by using LaSalle's theorem, it can be shown that $(e, \dot{e}, \eta) = 0$ is asymptotically stable.

4.2: Simulation Results

The simulation results for the closed-loop operation of the electrostatic micro-relay under the Lyapunov control design are shown in Figure 4.1. The desired electrode position y_d was set to (22). As a result, the control input was switched between (28) and (33) according to the profile described by (22). The control gains were selected as $c_1 = 0.3$, $c_2 = 0.3$, and $c_3 = 0.002$. From Figure 4.1, a fair improvement in the micro-relay performance can be seen, namely, the pull-in phenomenon disappeared as a closer inspection of the velocity plot (Figure 4.2) shows that the profile of the velocity corresponding to the closing of the relay is actually parabolic, and not impulse-like, as is the case for the open-loop operation shown in Figure 3.2. Despite the underdamped response, the settling time during opening is noticeably shorter than the open-loop one. It is also noted that no gain selection was capable of eliminating the oscillations during the micro-relay opening. Finally, it is noted that one now has significantly more control over the electrostatic charge, eliminating the delay in the response associated with the open-loop operation.

On the other hand, we were not able to operate the electromagnetic micro-relay with the Lyapunov-based control.

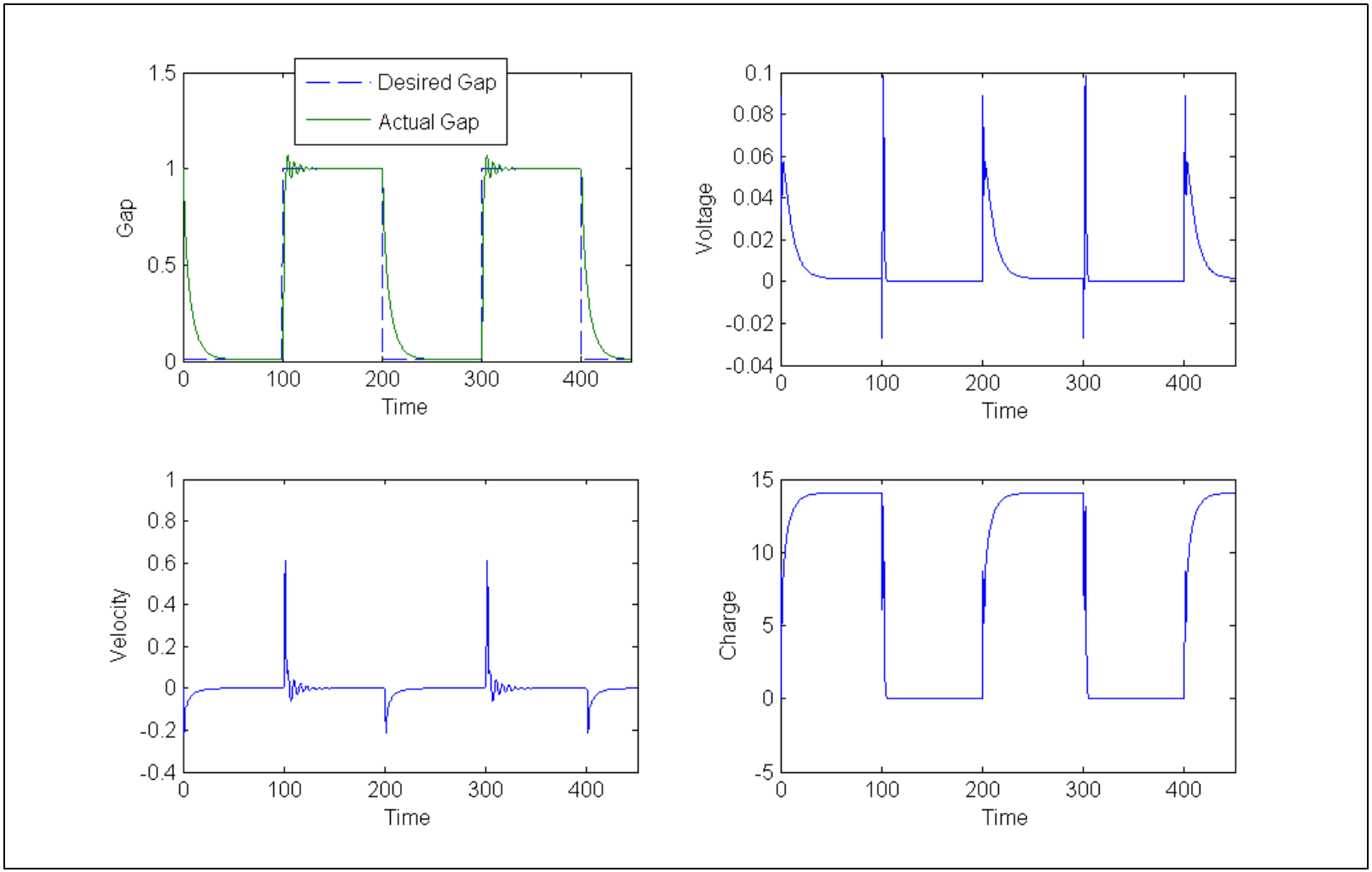

Figure 4.1. Electrostatic micro-relay operation with Lyapunov-based control

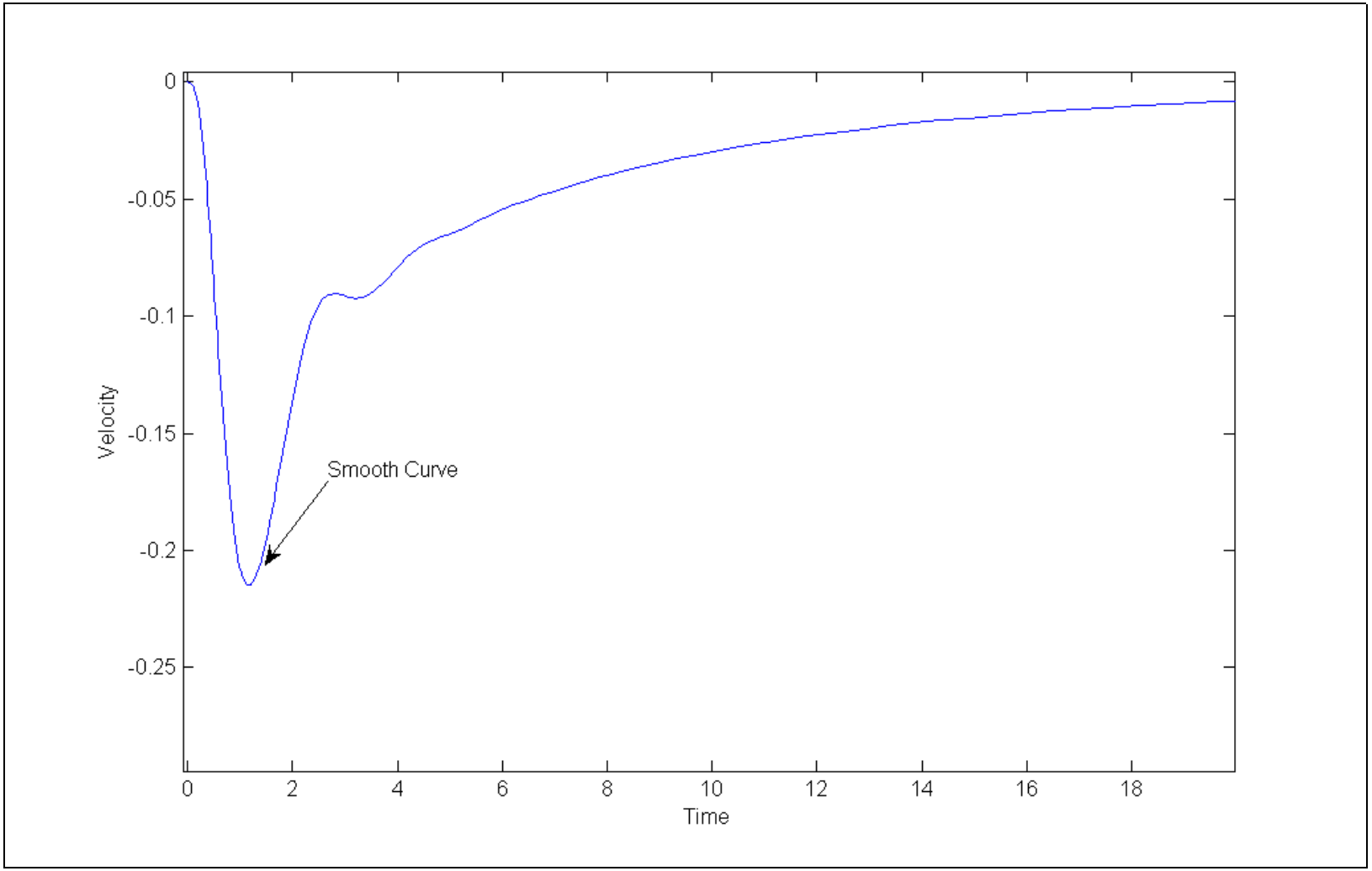

Figure 4.2. A close-up of the velocity of the plunger of the electrostatic micro-relay during closed-loop operation with Lyapunov-based control

Chapter 5: Feedback Linearization-Based Control

Due to the controller's unsatisfactory transient performance of the Lyapunov design during the electrostatic micro-relay opening and the inability to operate the electromagnetic micro-relay, in this section, an attempt is made to overcome these problems by constructing a feedback controller via the feedback linearization approach [8].

5.1: Control Synthesis

5.1.1: Input-Output Linearization

Before one can test for input-output linearizability, the generalized system (16) is transformed into standard state-space form. First, the coordinates are defined in the following manner:

$$\boldsymbol{x} := \begin{bmatrix} x_1 \\ x_2 \\ x_3 \end{bmatrix} := \begin{bmatrix} x \\ \dot{x} \\ z \end{bmatrix} \tag{36}$$

Standard space-state form is then

$$\begin{aligned} \dot{\boldsymbol{x}} &= f(\boldsymbol{x}) + g(\boldsymbol{x})u \\ y &= \vartheta(\boldsymbol{x}) \end{aligned} \tag{37}$$

where

$$f(\boldsymbol{x}) = \begin{bmatrix} x_2 \\ \frac{1}{m}(\alpha {x_3}^2 - b x_2 - k x_1) \\ \frac{-\gamma}{\beta}(g_0 - x_1) x_3 \end{bmatrix}, \quad g(\boldsymbol{x}) = \begin{bmatrix} 0 \\ 0 \\ 1 \end{bmatrix}, \quad \text{and} \quad \vartheta(\boldsymbol{x}) = x_1$$

Differentiating the output with respect to time until control-dependency appears is done as shown in (38).

$$\dot{y} = \frac{d\,\vartheta(\boldsymbol{x})}{d\,\boldsymbol{x}}\dot{\boldsymbol{x}} = \frac{d\,\vartheta(\boldsymbol{x})}{d\,\boldsymbol{x}}\left[f(\boldsymbol{x}) + g(\boldsymbol{x})u\right] = L_f\vartheta(\boldsymbol{x}) + \cancel{L_g\vartheta(\boldsymbol{x})u} = L_f\vartheta(\boldsymbol{x}) = \varphi_1(\boldsymbol{x}) \tag{38a}$$

$$\ddot{y}=\frac{d\,\varphi_1(\boldsymbol{x})}{d\,\boldsymbol{x}}\dot{\boldsymbol{x}}=\frac{d\,\varphi_1(\boldsymbol{x})}{d\,\boldsymbol{x}}\left[f(\boldsymbol{x})+g(\boldsymbol{x})u\right]=L_f\varphi_1(\boldsymbol{x})+\cancel{L_g\varphi_1(\boldsymbol{x})u}=L_f\varphi_1(\boldsymbol{x})=\varphi_2(\boldsymbol{x}) \tag{38b}$$

$$\dddot{y}=\frac{d\,\varphi_2(\boldsymbol{x})}{d\,\boldsymbol{x}}\dot{\boldsymbol{x}}=\frac{d\,\varphi_2(\boldsymbol{x})}{d\,\boldsymbol{x}}\left[f(\boldsymbol{x})+g(\boldsymbol{x})u\right]=L_f\varphi_2(\boldsymbol{x})+L_g\varphi_2(\boldsymbol{x})u=\varphi_3(\boldsymbol{x}) \tag{38c}$$

Note that only after the third differentiation does the dependence on the control input appear, where $L_g\varphi_2(\boldsymbol{x})\neq 0\ \forall\ x_3\neq 0$, indicating that the system in (37) has a *relative degree*, $\rho=3$ in D where $D:=\{\boldsymbol{x}:x_3\in(-\infty,0)\cup(0,\infty)\}$. Since the order of the system, n, is equal to the relative degree, then for every $\boldsymbol{x}_0\in D$, a neighborhood G of $\boldsymbol{x}_0$ exists such that the following map of $T(\boldsymbol{x})$ is a diffeomorphism on G:

$$T(\boldsymbol{x})=\begin{bmatrix}\vartheta(\boldsymbol{x})\\ L_f\vartheta(\boldsymbol{x})\\ L_f{}^2\vartheta(\boldsymbol{x})\end{bmatrix}=\begin{bmatrix}x_1\\ x_2\\ \frac{1}{m}(\alpha x_3{}^2-b\,x_2-k\,x_1)\end{bmatrix}=\begin{bmatrix}\zeta_1\\ \zeta_2\\ \zeta_3\end{bmatrix} \tag{39}$$

Therefore, the system is input-output linearizable on $D\ \forall\ x_3\neq 0$. Having such a restricted linearizability could cause a problem. However, it will be shown later that it has no effect on the control process.

The system dynamics in the new coordinates become

$$\dot{\boldsymbol{\zeta}}=\begin{bmatrix}\zeta_2\\ \zeta_3\\ \frac{2\alpha x_3}{m\beta}\left(u-\gamma(g_0-\zeta_1)x_3-\frac{b\zeta_3}{2\alpha x_3}-\frac{\beta k\zeta_1}{2\alpha x_3}\right)\end{bmatrix} \tag{40}$$

$$y=\zeta_1$$

5.1.2: Controller Design

After linearizing the system in the previous subsection, a simple linear state-feedback controller can be designed to improve the performance of the system. To start, consider a C^3 desired trajectory for the movable electrode $y_d(t)$, and let the tracking error be defined as shown in (41).

$$\boldsymbol{e} := \boldsymbol{\zeta} - \begin{bmatrix} y_d \\ \dot{y}_d \\ \ddot{y}_d \end{bmatrix} \tag{41}$$

It follows that the tracking error dynamics are given by

$$\dot{\boldsymbol{e}} = \begin{bmatrix} e_2 \\ e_3 \\ \dfrac{2\alpha x_3}{m\beta}\left(u - h(\zeta_1)x_3 - \dfrac{b\zeta_3}{2\alpha x_3} - \dfrac{\beta k \zeta_1}{2\alpha x_3}\right) - \ddot{y}_d \end{bmatrix} \tag{42}$$

The feedback linearization tracking control is then designed as

$$u = \gamma(g_0 - \zeta_1)x_3 + \frac{b\zeta_3}{2\alpha x_3} + \frac{\beta k \zeta_1}{2\alpha x_3} + \frac{m\beta}{2\alpha x_3}(\dddot{y}_d + \nu) \tag{43}$$

where $\nu = \boldsymbol{K}\boldsymbol{e}$, with $\boldsymbol{K} \in \mathbb{R}^{1\times 3}$ being a constant matrix, is any linear state feedback controller that stabilizes the resulting closed-loop linear system. The resulting error dynamics then become

$$\dot{\boldsymbol{e}} = (\boldsymbol{A} + \boldsymbol{B}\boldsymbol{K})\boldsymbol{e} \tag{44}$$

where

$$\boldsymbol{A} = \begin{bmatrix} 0 & 1 & 0 \\ 0 & 0 & 1 \\ 0 & 0 & 0 \end{bmatrix}, \quad \boldsymbol{B} = \begin{bmatrix} 0 \\ 0 \\ 1 \end{bmatrix}, \quad \text{and} \quad \boldsymbol{K} = \begin{bmatrix} K_1 & K_2 & K_3 \end{bmatrix}$$

Assigning closed loop eigenvalues of $(\sigma_1 = -a, \sigma_2 = -b, \sigma_3 = -c)$, one can obtain the characteristic equation of the closed-loop system as shown in (45).

$$(\sigma + a)(\sigma + b)(\sigma + c) = \sigma^3 + (a+b+c)\sigma^2 + (ac + bc + ab)\sigma + abc \tag{45}$$

The characteristic equation is also obtained from (44) as shown in (46). Equating the coefficients corresponding to the same order σ, yields the $\boldsymbol{K}$ matrix shown in (47). As shown, the values of $\boldsymbol{K}$ are written in terms of the desired eigenvalues.

$$|\sigma \boldsymbol{I}_3 - (\boldsymbol{A} + \boldsymbol{B}\boldsymbol{K})| = \sigma^3 - K_3\sigma^2 - K_2\sigma - K_1 \tag{46}$$

$$\boldsymbol{K} = [-abc \quad -(ac+bc+ab) \quad -(a+b+c)] \tag{47}$$

The micro-relay control problem is usually set up as a regulation/setpoint problem; i.e., the command is a piecewise constant function as in (22). However, the tracking controller shown in (43) gives one the flexibility to select a desired trajectory $y_d(t)$ that can potentially minimize damage to the micro-relay, since it has control over the *jerk* of the motion, $(\dddot{y}_d(t))$. A smooth trajectory should be selected to minimize both the velocity of the movable electrode as it approaches the fixed electrode during closing, and the overshoots during opening. This will be accounted for in the simulation results of this chapter.

5.1.3: Singularity Issue

The restricted input-output linearizability could potentially have a singularity at $x_3 = 0$. As Zhu explains in [21], this only happens when the system is at rest ($x = 0$), i.e., the micro-relay is opened. Since (37) with $u = 0$ is locally asymptotically stable about the origin, if necessary, one can set $u = 0$ when close to the origin to avoid the singularity. However, in this section, it is shown that for the case when $\dddot{y}_d = 0$, the singularity can also be avoided by the right choice of eigenvalues.

Consider the new coordinates dynamics as shown in (40). One can solve for $\boldsymbol{\zeta}$ in the manner shown in (48).

$$\boldsymbol{\zeta}(t) = L^{-1}\{(s\boldsymbol{I_3} - (\boldsymbol{A} + \boldsymbol{B}\boldsymbol{K}))^{-1}\}\boldsymbol{\zeta}(0) \tag{48}$$

where

$\zeta_j(t) = \sum_{i=1}^{3} c_{ji} e^{(-\sigma_i t)}$, $\sigma_i > 0$ corresponds to the i^{th} eigenvalue, and $j = 1,2,3$

Now, considering the control input (43) with $\dddot{y}_d = 0$, the remaining three terms are shown to be bounded in the manner illustrated in (49).

$$\frac{\zeta_1}{x_3}=\frac{\sum_{i=1}^{3} c_{1i}e^{-\sigma_i t}}{\sqrt{m\sum_{i=1}^{3} c_{3i}e^{-\sigma_i t}+b\sum_{i=1}^{3} c_{2i}e^{-\sigma_i t}+k\sum_{i=1}^{3} c_{1i}e^{-\sigma_i t}}}\leqslant\frac{\sum_{i=1}^{3} c_{1i}e^{-\sigma_i t}}{\sqrt{k}\sqrt{\sum_{i=1}^{3} c_{1i}e^{-\sigma_i t}}}\leqslant\frac{4c_{1,max}e^{-\sigma_{min}t}}{\sqrt{4k\,c_{1,min}e^{-\sigma_{max}t}}} \tag{49}$$

$$\frac{\zeta_1}{x_3}\leqslant\frac{2c_{1,max}}{\sqrt{k}\sqrt{c_{1,min}}}\frac{e^{-\sigma_{min}t}}{e^{-(\sigma_{max}/2)t}}\ \rightarrow\ \sigma_{max}\leqslant 2\sigma_{min}$$

Repeating this process with the remaining two terms leads to the same sufficient condition being imposed on the maximum and minimum eigenvalues. Therefore, to avoid the singularity in the system, one must choose the eigenvalues to satisfy the above sufficient condition.

5.2: Simulation Results

In simulating the feedback linearization control, the desired trajectory $y_d(t)$ is a filtered version of the one in (22). Specifically, let ψ equal the right-hand side of (22). Then, the desired trajectory is obtained from the dynamical system shown in (50).

$$\dot{\boldsymbol{\xi}}=\begin{bmatrix}0 & 1 & 0\\ 0 & 0 & 1\\ -10\lambda^3 & -21\lambda^2 & -12\lambda\end{bmatrix}\boldsymbol{\xi}+\begin{bmatrix}0\\0\\10\lambda^3\end{bmatrix}\psi \tag{50}$$

where

$$\boldsymbol{\xi}=\begin{bmatrix}y_d\\ \dot{y}_d\\ \ddot{y}_d\end{bmatrix},\quad \boldsymbol{\xi}(0)=\begin{bmatrix}1\\0\\0\end{bmatrix},\quad \text{and}\quad \lambda=0.35$$

The control matrix $\boldsymbol{K}$ was designed so the eigenvalues of the closed-loop system are located at (-3.5,-3.5,-4), which satisfies the condition in (49). The simulations for the electrostatic and electromagnetic micro-relays are shown in Figures 5.1 and 5.2 respectively. Again, the pull-in phenomenon was avoided during closing and more importantly, the opening of the micro-relay did not exhibit any overshoots or oscillations. Furthermore, due to the good tracking of the desired trajectory, the

opening operation exhibited a very short settling time. Thus, the transient performance during the micro-relay opening was vastly improved.

The effect of implementing a full-tracking controller, as opposed to a position-tracking one, is readily shown in Figure 5.3 which shows the micro-electrostatic relay during release, both with position-tracking and full-tracking control. As expected, it is apparent that full-tracking control leads to a better tracking of the command signal given and that is why it was adopted in this work.

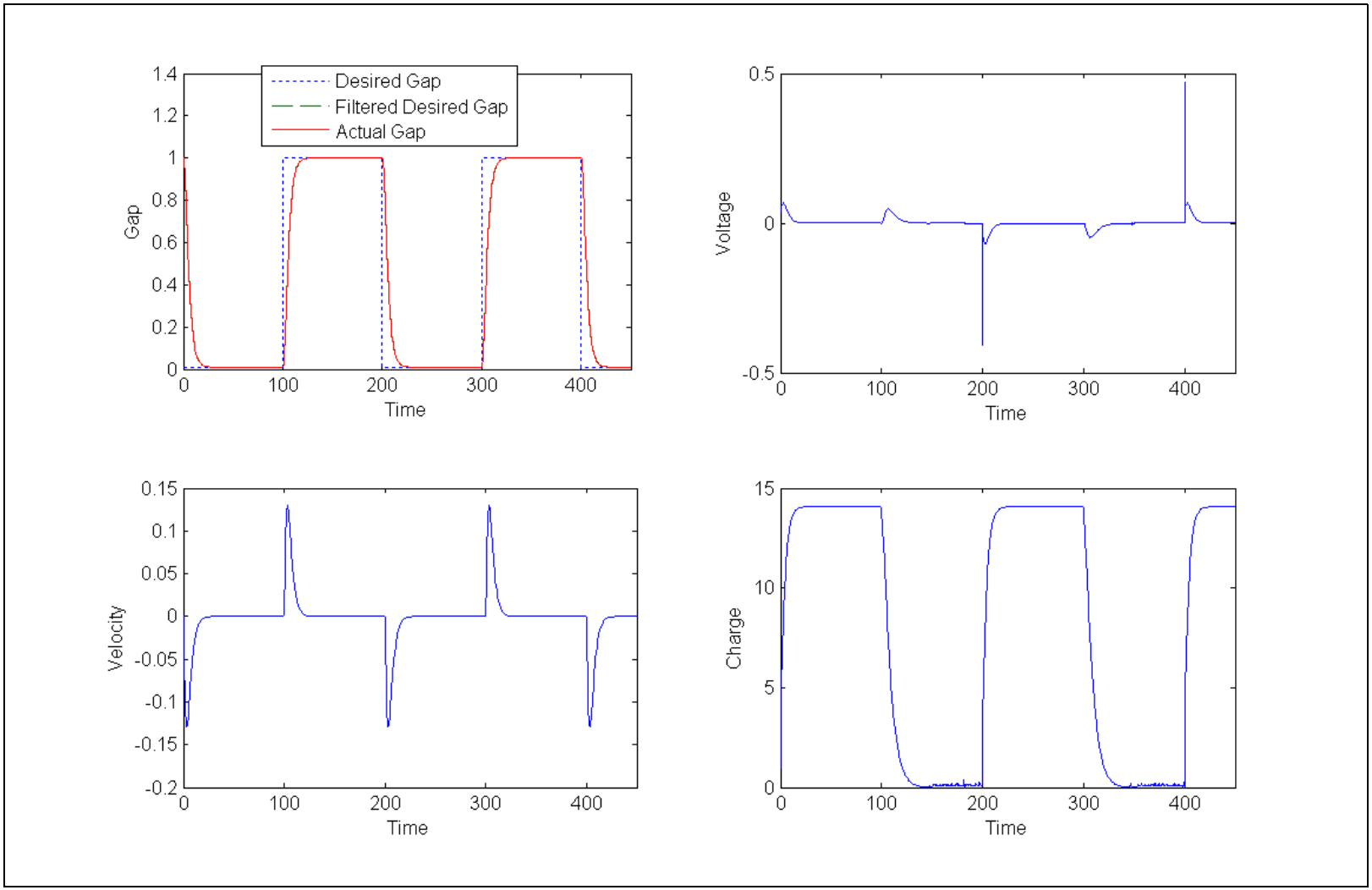

Figure 5.1. Electrostatic micro-relay operation with feedback linearization-based control

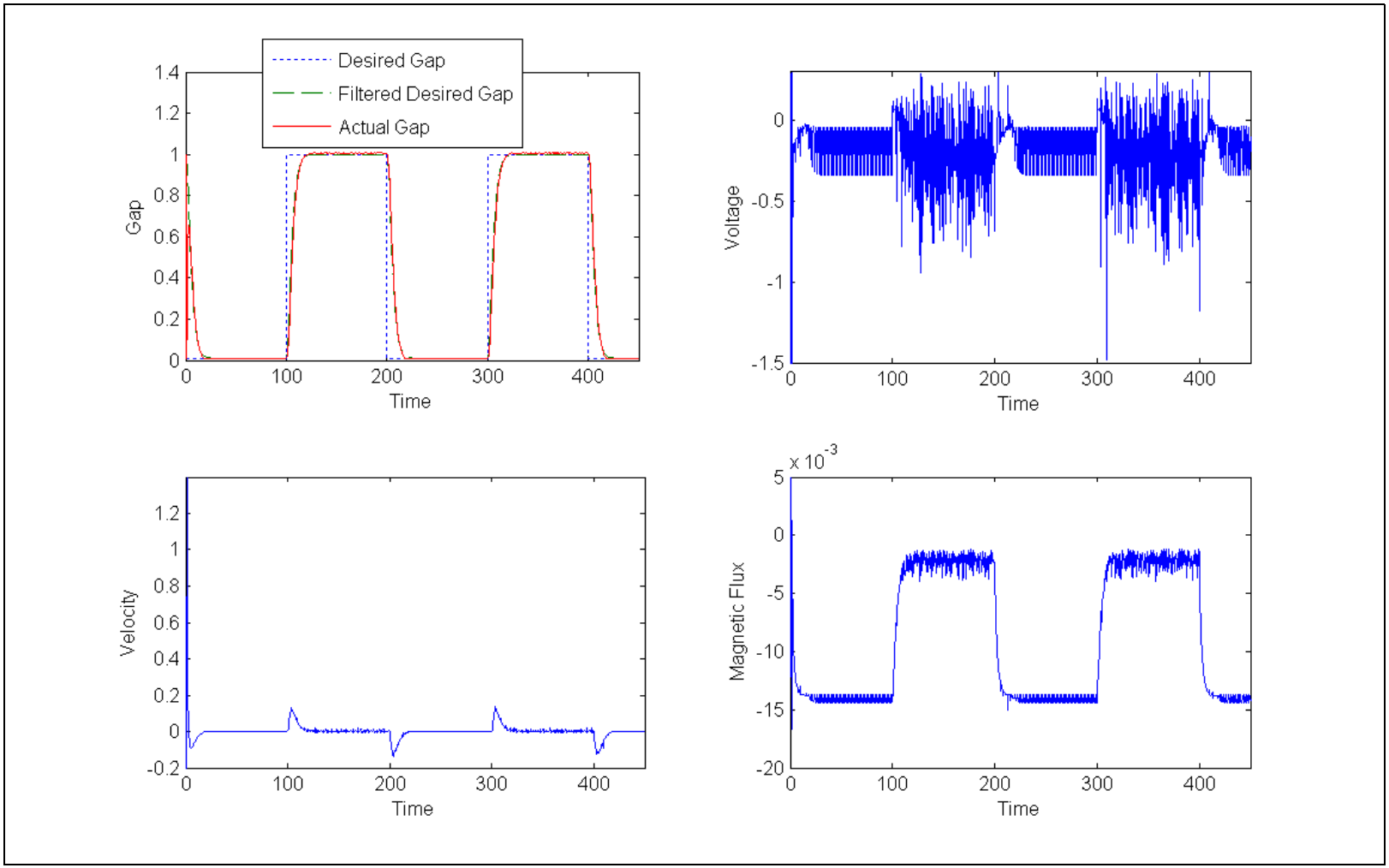

Figure 5.2. Electromagnetic micro-relay operation with feedback linearization-based control

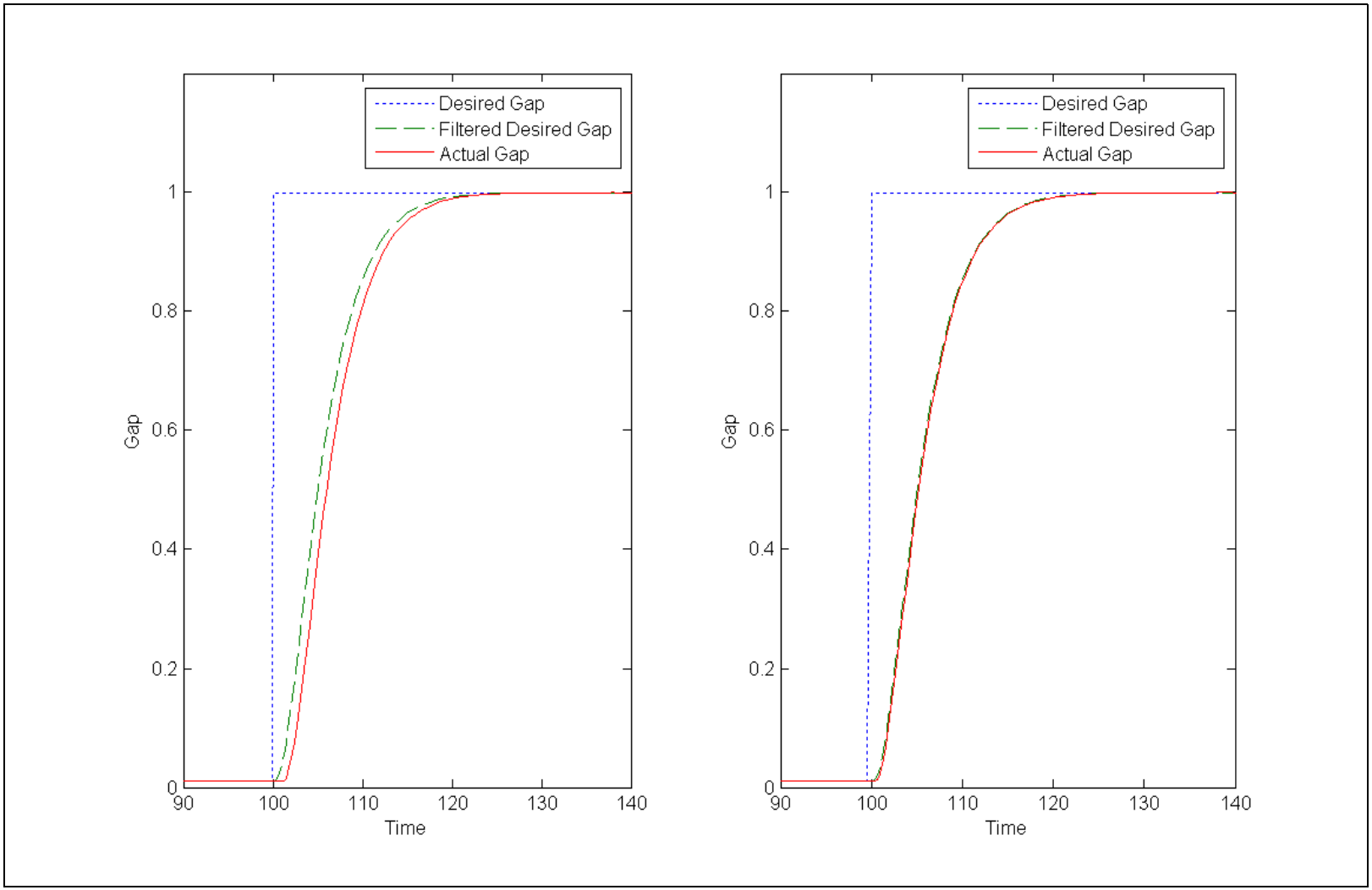

Figure 5.3. Electrostatic micro-relay operation with feedback linearization-based control with position-tracking (left) and full-tracking (right).

Chapter 6: Conclusions and Future Recommendations

It was illustrated that voltage-controlled electrostatic and electromagnetic micro-relays are subject to the same nonlinear phenomena when operated with open-loop control. This allowed for the formulation of a generalized control approach to eliminate pull-in and reduce transient response and settling times. Two feedback control schemes were examined in this work. The Lyapunov setpoint design eliminated pull-in, but yielded an unsatisfactory transient response during the micro-relay opening. The feedback linearization full-tracking design, on the other hand, significantly improved the transient response by eliminating the overshoots during opening while also avoiding pull-in. Both designs outperformed the uncontrolled (open-loop) operation, as expected.

For future work on this project, it is recommended that the model be made more complete by incorporating the nonlinear damping that is dependent on the gap between the two electrodes. Whether a solid plunger design or one with perforated holes is used, the effects of *squeezed-film* damping will have an effect on the relay's performance and should be accounted for. In addition, it is also recommended that the contact-bounce of the plates is taken into consideration, as it causes the bottom plate to oscillate whether the relay closes fully or is set to a minimum gap spacing. Finally, future work on this project should also involve the experimental setup and implementation of this control design.

Bibliography

[1] S. Bhansali, A.L. Zhang, R.B. Zmood, P.E. Jones, and D.K. Sood, "Prototype Feedback-Controlled Bidirectional Actuation System for MEMS Applications," *J. Microelectromech. S*, Vol. 9, No. 2, pp. 245-251, 2000.

[2] B. Borovic, C. Hong, A.Q. Liu, L. Xie, and F.L. Lewis, "Control of a MEMS Optical Switch," *Proc. Conf. Decision and Control*, pp. 3039-3044, Paradise Island, Bahamas, 2004.

[3] I.J. Busch-Vishniac, *Electromechanical Sensors and Actuators*, New York, NY: Springer-Verlag, 1999.

[4] I.J. Busch-Vishniac, "The Case for Magnetically Driven Microactuators," *Sensors and Actuators A*, No. 33, pp. 207-220, 1992.

[5] H.Guckel, T. Earles, J. Klein, J.D. Zook, and T. Ohnstein, "Electromagnetic Linear Actuators with Inductive Position Sensing," *Sensors and Actuators a*, No. 53, pp. 386-391, 1996.

[6] H. Hosaka, H. Kuwano, and K. Yanagisawa, "Electromagnetic Microrelays: Concepts and Fundamental Characteristics," *Sensors and Actuators A,* No. 40, pp. 41-47, 1994.

[7] S.J. Jeong, *UV-LIGA Micro-Fabrication of Inertia Type Electrostatic Transducers and Their Applications*, Ph.D. Dissertation, Louisiana State University, 2005.

[8] H. Khalil, *Nonlinear Systems*, Upper Saddle River, NJ: Prentice Hall, 2002.

[9] M. Krstic, I. Kanellakopoulos, and P. Kokotovic, *Nonlinear and Adaptive Control Design*, New York, NY: John Wiley & Sons, 1995.

[10] D.H.S. Maithripala, J.M. Berg, and W.P. Dayawansa, "Capacitive Stabilization of an Electrostatic Actuator: An Output Feedback Viewpoint," *Proc. American Control Conf.*, pp. 4053-4058, Denver, CO, 2003.

[11] D.H.S. Maithripala, J.M. Berg, and W.P. Dayawansa, "Control of an Electrostatic Microelectromechanical System Using Static and Dynamic Output Feedback," *ASME J. Dynamic Systems, Measurement, and Control*, Vol. 127, No. 3, pp. 443-450, 2005.

[12] D.H.S. Maithripala, J.M. Berg, and W.P. Dayawansa, "Nonlinear Dynamic Output Feedback Stabilization of Electrostatically Actuated MEMS," *Proc. Conf. Decision and Control*, Vol. 1, pp. 61-66, Maui, HI, 2003.

[13] D.H.S. Maithripala, B.D. Kawade, J.M. Berg, and W.P. Dayawansa, "A General Modeling and Control Framework for Electrostatically Actuated Mechanical Systems," *Intl. J. Robust and Nonlinear Control*, Vol. 15, pp. 839-857, 2005.

[14] S. Majumdar, N.E. McGruer, G.G. Adams, A. Zavracky, P.M. Zavracky, R.H. Morrison, and J.

Krim, “Study of Contacts in an Electrostatically Actuated Microswitch,” *Proc. Holm Conf. Electrical Contacts*, pp. 127-132, Arlington, VA, 1998.

[15] B. McCarthy, G.G. Adams, N.E. McGruer, and D. Potter, “A Dynamic Model, Including Contact Bounce, of an Electrostatically Actuated Microswitch,” *J. Microelectromechanical Systems*, Vol. 11, No. 3, pp. 276-283, 2002.

[16] F. Michel and W. Ehrfeld, “Mechatronic Micro Devices,” *Proc. Int. Symposium Micromechatronics and Human Science,* pp. 27-34, Nagoya, Japan, 1999.

[17] R. Nadal-Guardia, A. Dehé, R. Aigner, and L.M. Castañer, “Current Drive Methods to Extend the Range of Travel of Electrostatic Microactuaors Beyond the Voltage Pull-In Point,” *J. Microelectromechanical Systems*, Vol. 11, No. 3, pp. 255-263, 2002.

[18] S.D. Senturia, *Microsystem Design*, New York, NY: Springer, 2004.

[19] L. Wang, J.M. Dawson, P. Famouri, and L.A. Hornak, “Stroke-Length Control of a MEMS Device,” *Proc. Int. Symposium Industrial Electronics*, Vol. 2, pp. 535-539, Cholula, Mexico.

[20] J.D. Williams, *Design and Fabrication of Electromagnetic Micro-Relays Using the UV-LIGA Technique*, Ph.D. Dissertation, Louisiana State University, 2004.

[21] G. Zhu, J. Lévine, and L. Praly, “Improving the Performance of an Electrostatically Actuated MEMS by Nonlinear Control: Advances and Comparison,” *Proc. Conf. Decision and Control*, pp. 7534-7539, Seville, Spain, 2005.

[22] G. Zhu, J. Penet, and L. Saydy, “Robust Control of an Electrostatically Actuated MEMS in the Presence of Parasitics and Parameter Uncertainties,” *Proc. American Control Conf.*, pp. 1233-1238, Minneapolis, MN, 2006.

Vita

Younis, Mohamed was born in El-Minya, Egypt, on October 1st, 1984. Mohamed came to the United States to pursue his higher education and joined Louisiana State University in August, 2001. In May of 2005, he completed his Bachelor of Science in Mechanical Engineering. Mohamed joined the graduate program of LSU in June of 2005 and is expected to receive his Master of Science in Mechanical Engineering in December of 2006.

Mohamed is the younger son of Abdelrahman Younis and Sanaa Ibrahim and has a brother, Ahmed Younis.